Pharm Res (2016) 33:510–525
DOI 10.1007/s11095-015-1806-z

RESEARCH PAPER

A Comparison of the Pharmacokinetics and Pulmonary Lymphatic Exposure of a Generation 4 PEGylated Dendrimer Following Intravenous and Aerosol Administration to Rats and Sheep

Gemma M. Ryan[1] • Robert J. Bischof[2] • Perenlei Enkhbaatar[3] • Victoria M. McLeod[1] • Linda J. Chan[1] • Seth A. Jones[1,4] • David J. Owen[4] • Christopher J. H. Porter[1] • Lisa M. Kaminskas[1]

Received: 10 July 2015 / Accepted: 6 October 2015 / Published online: 20 October 2015

ABSTRACT

Purpose Cancer metastasis to pulmonary lymph nodes dictates the need to deliver chemotherapeutic and diagnostic agents to the lung and associated lymph nodes. Drug conjugation to dendrimer-based delivery systems has the potential to reduce toxicity, enhance lung retention and promote lymphatic distribution in rats. The current study therefore evaluated the pharmacokinetics and lung lymphatic exposure of a PEGylated dendrimer following inhaled administration.

Methods Plasma pharmacokinetics and disposition of a 22 kDa PEGylated dendrimer were compared after aerosol administration to rats and sheep. Lung-derived lymph could not be sampled in rats and so lymphatic transport of the dendrimer from the lung was assessed in sheep.

Results Higher plasma concentrations were achieved when dendrimer was administered to the lungs of rats as a liquid instillation when compared to an aerosol. Plasma pharmacokinetics were similar between sheep and rats, although some differences in disposition patterns were evident. Unexpectedly, less than 0.5% of the aerosol dose was recovered in pulmonary lymph.

Conclusions The data suggest that rats provide a relevant model for assessing the pharmacokinetics of inhaled macromolecules prior to evaluation in larger animals, but that the pulmonary lymphatics are unlikely to play a major role in the absorption of nanocarriers from the lungs.

KEY WORDS lymphatic · pharmacokinetics · pulmonary · rats · sheep

ABBREVIATIONS

BALF	Bronchoalveolar lavage fluid
CMLD	Caudal mediastinal lymph duct
CMLN	Caudal mediastinal lymph node
MØ	Alveolar macrophages
SEC	Size exclusion chromatography

INTRODUCTION

Inhaled administration of drugs and therapeutic macromolecules has potential as a non-invasive route of systemic or local (lung) delivery. Administration of therapeutics directly to the lungs may also provide high local concentrations at the site of action thereby enhancing the treatment of respiratory disease. For many small molecule therapeutics, however, the physiology of the lungs (high surface area, thin epithelium, high blood perfusion, near sink conditions) drives rapid absorption of drug into the systemic circulation, limiting local exposure and activity within the lungs [1]. Rapid systemic absorption may be ideal for the treatment of systemic conditions that require an immediate onset of action, but slowing the rate of absorption has the potential to provide more sustained plasma exposure and to prolong the duration of therapeutic activity [2]. To this end, association (through covalent conjugation or non-covalent entrapment) of therapeutics with macromolecular drug-carriers has been employed previously to manipulate the pharmacokinetic behavior of small molecule therapeutics

✉ Lisa M. Kaminskas
lisa.kaminskas@monash.edu

[1] Drug Delivery, Disposition and Dynamics, Monash Institute of Pharmaceutical Sciences, Monash University, 381 Royal Pde, Parkville, VIC 3052, Australia

[2] Biotechnology Research Laboratories, School of Biomedical Sciences, Monash University, Clayton, VIC 3800, Australia

[3] Department of Anaesthesiology, University of Texas Medical Branch, 301 University Boulevard, Galveston, Texas 77555, USA

[4] Starpharma Pty Ltd, 4/6 Southhampton Cresent, Abbotsford, VIC 3067, Australia

[3] and to improve the stability of drugs and proteins in the lungs [4, 5].

Drug association with nanometer-sized drug carriers (nanocarriers) provides a potential means of delivering drugs, including cancer chemotherapeutics, directly to the lungs for the improved treatment of lung resident disease and to control pulmonary residence time and the rate of drug release. Further potential utility may be found in refining the design of inhalable drug carriers in order to target the pulmonary lymphatic system and to better treat diseases that reside within the lung lymphatics, such as pulmonary lymphoma, lung-resident lymph node metastases and lymphangitis carcinomatosa. The targeted delivery of contrast agents to the lung lymphatics also provides an opportunity to stage lung cancers without the need for invasive surgical procedures.

Selective delivery of drugs to lung resident cancers and the pulmonary lymphatic system following inhaled administration has the potential to limit systemic exposure when compared to the conventional intravenous (IV) delivery of chemotherapeutic drugs. The toxic side effects of chemotherapeutic drugs may therefore be limited and larger doses administered to enhance the treatment of lung-resident disease. In support of this suggestion, a number of studies have previously demonstrated the ability of nanocarriers to target the lymphatic system following IV [6], subcutaneous (SC) [6–10], intradermal [11, 12] and intramuscular [13] administration.

Nanometer (~10 nm) sized dendritic polymers (dendrimers) show considerable potential as drug delivery systems after administration via IV, SC and pulmonary routes [14]. PEGylation of an otherwise polycationic dendritic scaffold can also be utilized to produce dendrimers with significantly reduced cell surface interactions due to the masking of surface charges and slower catabolism for polypeptide-based dendrimers due to the hindered access of peptidases and proteases to the scaffold [15, 16]. As such, previous work [17] has demonstrated that the pulmonary pharmacokinetics and *in vivo* stability of generation 4 poly(lysine) dendrimers in rats can be manipulated by modifying the molecular weight of polyethylene glycol (PEG) chains that are conjugated to the dendrimer surface to enhance biocompatibility. In this study, generation 4 dendrimers conjugated with low MW PEG chains (≤570 Da) were efficiently and rapidly (T_{max} within 24 h) absorbed from the lungs, whilst dendrimers conjugated with higher MW PEG (2200 Da) displayed limited (approximately 2%) and slow absorption from the lungs and more efficient mucociliary clearance. Furthermore, the dendrimer conjugated with 200 Da PEG (to give a 11 kDa dendrimer) was very rapidly degraded in the lungs such that much of the absorbed dose was due to the uptake of low MW fragments of dendrimer catabolism. Stability in the lungs was increased via the conjugation of increasing PEG MW. Of particular note, a 22 kDa PEGylated poly(lysine) dendrimer (generation 4) with complete surface conjugation of 570 Da PEG (i.e., 2 PEG chains per surface lysine) was shown to have approximately 30% bioavailability after liquid instillation into the lungs of rats, and to show little *in vivo* biodegradation [17]. This suggested relatively efficient absorption and access to the pulmonary interstitium as well as to the blood and lymph capillaries that reside along the deep lungs and conducting airways for PEGylated dendrimer of this size. The same dendrimer was also shown in an earlier study to be transported into the lymphatics after IV and SC administration to rats (12 and 29% of an IV and SC dose over 30 h respectively) [6]. Based on this data, we hypothesized that a significant proportion of the dendrimer may be systemically absorbed from the lungs via pulmonary lymphatic capillaries.

The *in vivo* evaluation of pulmonary drug and macromolecule pharmacokinetics is performed in the first instance in rodent models. This reflects the availability, well characterized physiology and low cost of rodents and the small quantities of drug required for administration and evaluation. Larger animal models, however, offer the potential to evaluate pulmonary pharmacokinetics in animals with a respiratory physiology that is more relevant to humans [18]. Although the number of published pharmacokinetic studies in larger animals such as sheep are limited, the physiological similarities between ovine (sheep) and human lungs have prompted the use of sheep as a model for studying various respiratory diseases and injury states [19–23]. Of particular relevance is the similar size and body weight of sheep and similar breathing rates and tidal volumes of sheep when compared to humans, in contrast to the very different lung dimensions and breathing patterns in rodents [20]. These factors play a critical role in the lung disposition of inhaled particles and may impact on pharmacokinetics and lung clearance kinetics and pathways [24]. Furthermore, and perhaps most alluringly, the large size of sheep allows for advanced surgical procedures to be performed that are not possible in rodents. For example, pulmonary lymph from rats cannot be sampled without a thoracotomy, a procedure that is difficult in rodents (the thoracic lymph duct drains into the systemic circulation beneath the clavicle and rib cage in rats). In contrast, a surgical method for the collection of pulmonary lymph from conscious sheep has previously been described [25].

In the current study, we used sheep to evaluate the contribution of the pulmonary lymphatic system to the systemic absorption of a 22 kDa PEGylated dendrimer after administration as a liquid aerosol dose to the lungs. This was achieved by cannulating the efferent caudal mediastinal lymph duct (CMLD) which collects most of the lymph formed within the lungs before deposition into the thoracic lymph. In addition, we sought to evaluate differences in the pharmacokinetic behavior of the PEGylated dendrimer between rats and sheep after IV and inhaled administration. Significantly, this work provides the first comparison between the pulmonary pharmacokinetics of a macromolecular drug delivery system in rats

and a large animal model, enabling some insight into the expected biopharmaceutical behavior of inhaled nanocarriers in humans. Previous studies to evaluate the pulmonary pharmacokinetics of PEGylated dendrimers in rats were performed following liquid instillation to the lungs, a method that is commonly used but results in differences in drug deposition in the lungs when compared to inhaled administration. The pulmonary pharmacokinetics of the dendrimer in rats was therefore first evaluated after liquid aerosol administration to the lungs using a Penn-Century microsprayer.

METHODS

Materials

A 22 kDa, poly-lysine dendrimer with complete PEG (570 Da) surface coverage (i.e., 2 PEG chains per surface lysine) ($lys_{16}(PEG_{570})_{32}$) (Fig. 1) was synthesized as previously described [15], except that in this case (to necessitate quantification in a larger animal), the radioactivity of the dendrimer was increased (2.7 μCi/mg) by incorporating a larger proportion of ^{3}H-lysine into the penultimate lysine layer [15]. $Lys_{16}(PEG_{570})_{32}$ was solubilized in sterile saline (50 mg/ml) and stored in working aliquots at −20°C until used.

Marcain® and heparin were purchased from Clifford Hallam Healthcare (VIC, Australia) and saline was purchased from Baxter (NSW, Australia). Oxytetracycline, procaine penicillin, and Lethabarb were obtained from Virbac (NSW, Australia). Fentanyl transdermal patches were from Janssen Pharmaceuticals Inc. (Beerse, Belgium) and Evans blue dye and hydrogen peroxide (30% *w/v*) were obtained from Sigma-Aldrich (MO, USA). Buprenorphine was from Reckitt Benckiser Healthcare (Berkshire, England). Irga-Safe Plus™ and Soluene® were from PerkinElmer (MA, USA) and isoflurane was from Delvet Pty Ltd (NSW, Australia). Isopropyl alcohol (IPA) was obtained from SSA Enterprises (KA, India). Chlorhexidine was from Livingstone International Healthcare (NSW, Australia). Thiopentone was obtained from Troy Laboratories (NSW, Australia). All other reagents were AR grade and were used without further purification. Polyethylene cannula (0.96 mm×0.58 mm) and polyvinyl cannula (1.5 mm×2.7 mm) were from Microtube Extrusions (NSW, Australia). Silastic cannula (0.63 mm×1.19 mm) was from Dow Corning (MI, USA).

Animals

Rats

Male Sprague–Dawley rats (260–315 g) were obtained from Monash Animal Services (VIC, Australia). Rats that underwent surgical procedures were fasted for 12 h prior to surgery and for up to 8 h following dendrimer administration. Food was freely available at all other times, and water was available *ad libitum*. Surgically cannulated rats were housed in metabolic cages for sample collection and during recovery from surgery, while non-cannulated rats were housed in groups of 3 in microisolator cages for the entirety of the study.

Sheep

Lung lymphatic pharmacokinetics was evaluated in female Merino sheep (22–43 kg). Female sheep were used since previous lymph duct cannulation procedures were performed in female sheep of this strain [26], and physiological variability has been known to occur between the lymphatic system of male and female animals [27]. Sheep were purchased from a Monash Animal Services approved breeding facility. Sheep were fasted for 24 h prior to surgical procedures and for 12 h prior to dosing. Food was freely available at all other times, and water was available *ad libitum*. Sheep were housed in metabolic cages during recovery from surgery and after surgical implantation for the entirety of the study to allow for sample collection.

All animals were housed under ambient conditions (20–22°C) and were maintained on a 12 h light/dark cycle. All rat and sheep experimentation was approved by the Monash Institute of Pharmaceutical Sciences Animal Ethics Committee, and conducted in accordance with the Australian Code of Practice for the Care and Use of Animals for Scientific Purposes.

Characterization of Intravenous and Pulmonary Pharmacokinetics in Rats

Rats were dosed in parallel groups and were administered dendrimer either via IV infusion (1 mg in 1 ml saline) over 2 min or via aerosol administration to the lungs (1 mg in 100 μl saline). We have previously characterized the IV pharmacokinetics of the dendrimer over 30 h [15]. In this study, the IV pharmacokinetics of the dendrimer was re-evaluated over 7 days to enable accurate comparison to sheep pharmacokinetic data that was similarly collected for 7 days. Methods were as described previously [17].

Rats that were administered aerosolized dendrimer to evaluate plasma pharmacokinetics and dendrimer disposition (Table I, group R1) were first cannulated via the right carotid artery as previously described to facilitate repeated blood collection in conscious, freely moving animals. Rats administered dendrimers via the IV route (Table I, group R2) were cannulated via both the carotid artery and the right jugular vein as previously described [16] to facilitate blood sampling and the IV infusion of the dendrimer solution respectively in

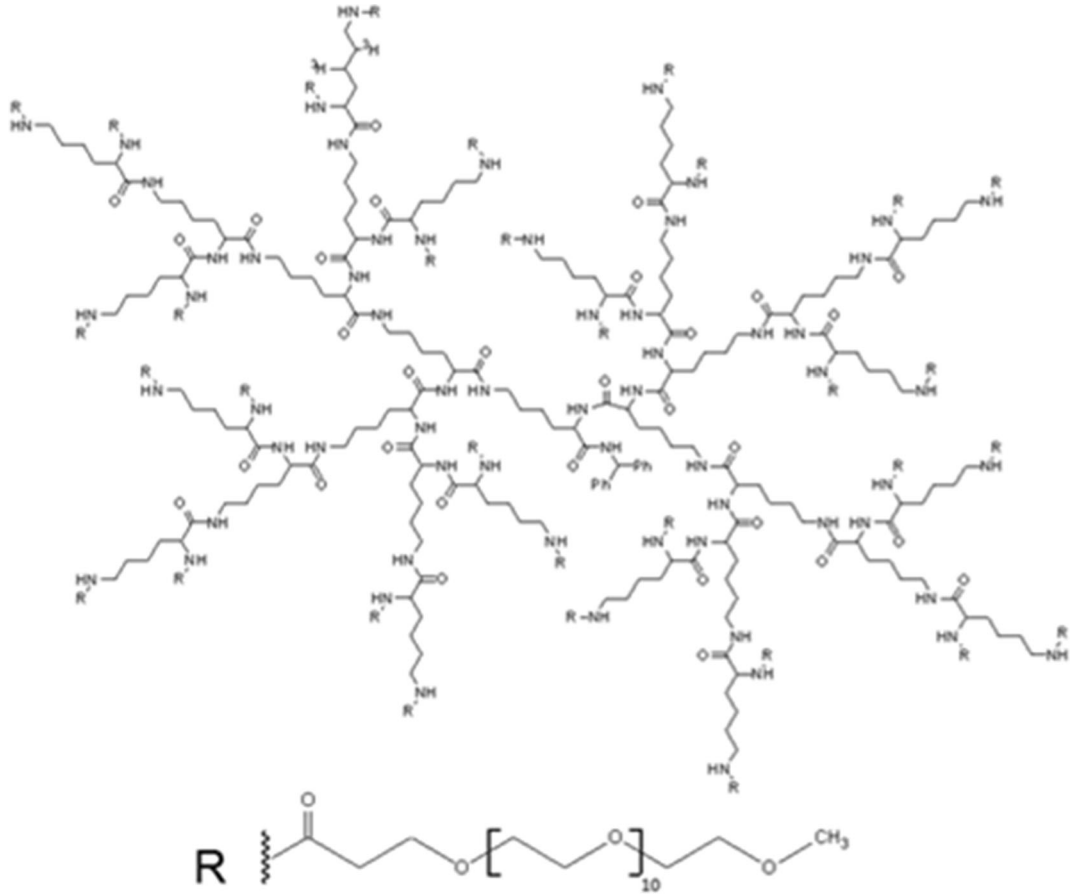

Fig. 1 PEGylated generation 4 poly(lysine) dendrimer. Adapted with permission from reference [17]. Copyright 2013 American Chemical Society.

conscious, freely moving animals. All surgical procedures were performed under isoflurane anesthesia, and Marcaine (0.25 mg in 50 μl) was administered SC to the surgical site(s) prior to incisions being made to provide local analgesia. Following surgical procedures, rats were connected to swivel-tether jackets [28] and housed in metabolism cages where they remained for the duration of the study. Rats were allowed to recover overnight prior to dendrimer administration.

Immediately prior to dendrimer administration, blank blood samples (150 μl) were collected into heparinized vials (10 I.U /vial) as previously described [16], and blank urine and feces samples were collected from each rat. For the IV group, a 1 ml solution of dendrimer (in sterile saline) was infused via the jugular vein cannula over 1.5 min. At the conclusion of the infusion, the jugular vein cannula was flushed with a further 0.3 ml saline over 30 s to flush any remaining dose into the rat. A t_0 blood sample (150 μl) was

Table I Animal Dosing and Sampling Outline

Species	Group	Animal numbers	Dosing route	Lymph duct cannulated?	Blood sampled?	Urine/ feces sampled	BALF sampled	Organs collected
Rat	R1	3	IV	No	Yes	Yes	168 h	Lungs, liver, spleen, kidneys
Rat	R2	4	Pulm	No	Yes	Yes	168 h	Lungs, liver, spleen, kidneys
Rat	R3	3× ($n=3$)	Pulm	No	No	No	1, 8 and 72 h	Lungs
Sheep	S1	3	IV	No	Yes	Yes	No	Lungs, liver, spleen, kidneys, node
Sheep	S2	3	Pulm	No	Yes	Yes	No	Lungs, liver, spleen, kidneys, node
Sheep	S3	4	Pulm	Yes	Yes	No	No	Nil
Sheep	S4	3	Pulm	No	No	No	0.5, 24, 72 and 168 h	Nil

collected immediately following the infusion. Rats administered dendrimer via the lungs were anesthetized under isoflurane and suspended via the front incisors in a supine position on a dosing board at an angle of 60° as previously described [17]. A 100 µl solution of dendrimer (in sterile saline) was loaded into a Penn-Century MSA-250-R MicroSprayer®/Syringe Assembly dosing device (Penn-Century, PA, USA; 16–22 µm particle size) as recommended by the manufacturer. A laryngoscope was used to guide the device down the trachea to a distance of 2.5 cm past the larynx, where the entire dose was expelled from the device in time with inhalation. The rat was removed from the dosing board and a t_0 blood sample (150 µl) was collected. Rats were held in an upright position until they regained consciousness prior to being returned to metabolism cages.

Further blood samples (150 µl) were collected from both IV and pulmonary dosed rats 0.5, 1, 2, 3, 4, 6, 8, 12, 24, 30, 48, 72, 96, 120, 144 and 168 h following dendrimer administration. Blood samples were centrifuged (3500*g*, 5 min) and plasma (80–100 µl) was collected and vortex mixed with Irga-Safe Plus™ scintillation fluid (1 ml) prior to determination of radiolabel content via liquid scintillation counting on a Packard Tri-Carb 2000CA liquid scintillation analyzer (Meriden, CT). Total urine and feces were collected from each rat for the entirety of the sampling period and were analyzed for ^{3}H content as previously described [15]. Following collection of the 168 h sample, rats were euthanized under isoflurane anesthesia via exsanguination from the carotid artery cannula. Bronchoalveolar lavage fluid (BALF) was collected from all rats post-mortem as previously described [17] to evaluate the proportion of the dose remaining in lung lining fluid. BALF was centrifuged (4500*g* for 5 min) to pellet the alveolar macrophages (MØ) which were resuspended in saline (1 ml). Both supernatant and pelleted MØ were analyzed for ^{3}H as previously described [17]. The lungs, liver, spleen and kidneys were also excised, weighed and analyzed for ^{3}H as previously described [15].

A separate cohort of rats were similarly dosed with dendrimer via the lungs (3 groups of $n=3$ rats per group) to generate disposition data after pulmonary administration. At different times after dosing rats were anaesthetized and a cannula inserted into the carotid artery as described previously [16]. At 1, 8 and 72 h post dose animals were euthanized via exsanguination under isoflurane as described above to assess lung retention and the stability of the dendrimer over time (Table I, group R3). BALF and lung tissue was collected and analyzed for ^{3}H content as described above.

Characterization of Intravenous and Pulmonary Pharmacokinetics in Sheep and Lung Lymphatic Exposure After Pulmonary Administration

Sheep were dosed in parallel groups with 100 mg dendrimer according to the scheme in Table I. Group S1) IV dosed, non-lymph cannulated; group S2) pulmonary dosed, non-lymph cannulated; group S3) pulmonary dosed and lymph-cannulated; and group S4) pulmonary dosed with no cannulation. Cannulas were surgically implanted into sheep 5–7 days prior to dendrimer administration. Sheep were initially anaesthetized via IV administration of thiopentone (20 mg/kg). They were then immediately intubated with an endotracheal tube which was connected to a mechanical ventilator to maintain anesthesia with isoflurane (2.5% in oxygen) during the surgery. Prior to incisions being made, sheep were injected with oxytetracycline (5 mg/kg) and procaine penicillin (2400 IU/kg) in the right hind flank to prevent infections during and post-surgery, and marcain (10–25 mg) was injected at the incision sites. Fentanyl patches (75 mg) were applied to the skin under the right leg to provide post-surgical analgesia for 3 days after surgery. Buprenorphine (0.005 mg/kg) was also injected into the leg muscle of sheep undergoing lymph duct cannulations to provide stronger analgesia for 8 h during and after surgery. Sheep in groups S1-3 had a venous catheter inserted into the right jugular vein to facilitate blood collection and IV dendrimer administration as previously described [29]. The patency of the cannulas was maintained by flushing the cannulas with heparinized saline (10 U/ml) daily and after blood sampling. Sheep that were used to provide lung lymph after pulmonary dosing (group S3) were subsequently cannulated via the efferent CMLD which drains the caudal mediastinal lymph node (CMLN) using a slight modification to a previously described method [25] where systemic lymph contributions to the CMLN were not removed prior to cannulation. Briefly, a thoracotomy was made in the 5th right intercostal space and the efferent CMLD was exposed, ligated and cannulated with autoclave sterilized silastic tubing. The tubing was then exteriorized through a small incision in the chest wall for the collection of lymph. Following surgery, sheep were fitted with thin elastic netting to prevent them from chewing or pulling on cannulas, and were allowed to recover from anesthesia in metabolic cages where they were housed for the remainder of the study. Sheep were allowed to recover for up to 7 days prior to dendrimer administration.

Immediately prior to dendrimer administration, 5 ml of blank blood was collected from the jugular vein cannula of sheep in groups S1-3 into 10 ml heparinized (500 IU) centrifuge tubes. Blank lymph samples were also collected into vials containing heparin (500 IU), and blank urine and feces were sampled. The separate collection of urine and feces from sheep was facilitated by the attachment of wire mesh to the bottom of the metabolism cages which enabled pellets of feces to roll into a separate bucket to that was used to collect urine (Fig. 2).

Sheep that were dosed intravenously (group S1) were administered dendrimer in sterile saline (3 ml) as an infusion via the jugular vein cannula over 1.5 min. A further 10 ml of heparinized saline was then flushed through the cannula over 30 s to ensure the entire dose was delivered to the sheep.

Following infusion, a t_0 and a 30 min blood sample (5 ml) were withdrawn into heparinized tubes.

Sheep that were dosed via the lungs (groups S2-4) were removed from metabolism cages and positioned in specialized restraining harnesses to restrict movement of the head and neck and to facilitate dendrimer administration and BALF sample collection. To facilitate dendrimer administration to the lungs, cuffed endotracheal tubes were lubricated with lignocaine gel and inserted down the trachea through the nasal passage. The dendrimer dosing solution (in 5 ml saline) was aerosolized via a Nomad Nex Gen Travel Nebulizer System (Allersearch, NJ, USA; mass median aerodynamic diameter 1.76 μm), and placed in line with a dual phase control respirator (Harvard Apparatus, MA, USA) that was set to 20 breaths per minute at 35% inspiration for 25 min. Hudson filters (Hudson RCl, NC, USA) were placed in the expiratory line to collect any expired dendrimer dose, and following dendrimer administration, all lines, filters and nebulizer components were rinsed with sterile saline to collect any remaining or expired dose. The proportion of the dendrimer dose not delivered to or retained in the lungs of sheep (i.e., dose remaining in the dosing device or tubing and expired dose) was determined via scintillation counting and then subtracted from the nominal dose administered to sheep in subsequent calculations.

Following dendrimer administration to the lungs, an initial blood sample was collected 30 min after the beginning of aerosol administration (t_0 blood sampling was not possible since administration of the dose took 25 min). Further blood samples were then collected from sheep in groups S1-3 at 1, 2, 4, 6, 8, 12, 24, 30, 48, 72, 96, 120, 144 and 168 h. Blood samples were centrifuged (3500*g* for 5 min) to pellet red blood cells and plasma was collected. Plasma (1–3 ml) was mixed with scintillation fluid (10 ml) and analyzed for radiolabel content via liquid scintillation counting. Lymph fluid was collected into heparinized vials or sterile heparinized (5000 U) 75 cm^2 cell culture flasks over the following collection times: 0–1, 1–2, 2–4, 4–6, 6–8, 8–12, 12–24, 24–48, 48–72, 72–96, 96–120, 120–144 and 144–168 h. Up to 5 ml of each lymph sample was centrifuged (3500*g*) to pellet cells. The supernatant was collected and vortexed with IRGA-Safe (10 ml) and analyzed for tritium content via liquid scintillation counting. The cell pellet was suspended in saline (1 ml) and stored at −20°C until further analysis. Cell pellets from lymph fluid were analyzed for tritium content in the same way as MØ (see below). Total feces and urine excreted by sheep in groups S1 and 2 were collected and weighed at 24 h intervals and analyzed for excreted ^3H as described below.

In addition to sheep that were used to evaluate the plasma pharmacokinetics and disposition of the dendrimer (groups S1-3), $n=3$ sheep (group S4) were administered dendrimer via the lungs and underwent BALF sampling at various time points over 7 days to evaluate the stability of the dendrimer in the lungs and to provide an estimate of the rate of dendrimer clearance from the lungs (similar to rats in group R3). In this group of sheep, a blank BALF sample was collected from a region of one lung lobe prior to dendrimer administration. Briefly, a fiber-optic endoscope was guided via the nasal canal into the right caudal lung lobe, and saline (30 ml) was administered via a polyethylene cannula fed to 5 cm past the distal end of the endoscope. Following instillation, saline was withdrawn from the lung (average 35% volume recovery) and the endoscope was removed. Sheep were subsequently administered dendrimer (100 mg) via nebulization as described above, and immediately following dendrimer administration another BALF sample was collected from the left caudal lung lobe. Further BALF samples were collected at 24, 72 and 168 h following dendrimer administration from alternating right and left caudal lung lobes.

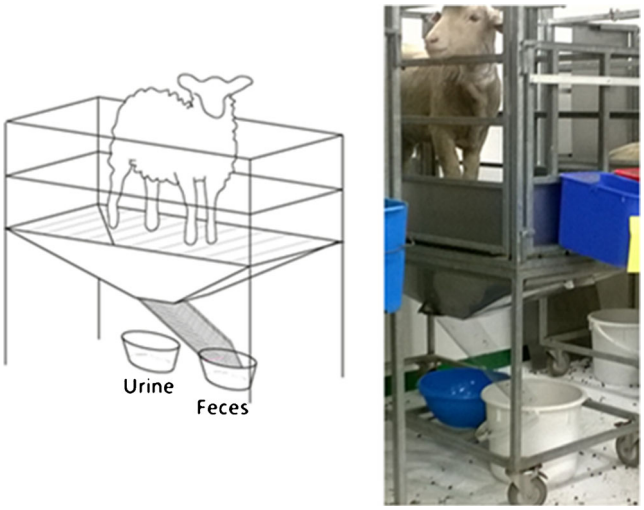

Fig. 2 Metabolism cage for the individual collection of urine and feces from sheep.

Up to 5 ml of BALF was centrifuged (4500*g*, 5 min) to pellet MØ which were reconstituted in saline (1.5 ml). MØ and BALF supernatant were stored at −20°C until analyzed. Radiolabel content in BALF and MØ was analyzed as described above.

At the end of the study, sheep were euthanized via a bolus injection of Lethabarb (20 ml) into the jugular vein cannula, or via intrajugular injection in the case of the uncannulated sheep in group S4. The lungs, liver, spleen, kidneys and CMLN from sheep in groups S1 and 2 were then collected and weighed. The entire lung and lymph node, and representative (approx. 10 g) samples of liver, spleen and kidneys were stored at −20°C until analyzed.

Organ Biodistribution in Sheep

Organs from sheep were analyzed for radiolabel content using a similar procedure to that reported for rat samples, with some modifications.

Urine: An aliquot (1 ml) of pooled urine collected over each 24 h time period was mixed with IRGA-Safe (15 ml) and analyzed via liquid scintillation counting.

Organs: Samples of liver, kidney, spleen and the entire CMLN were homogenized in water (approximately 5 ml) as described previously [16]. Total sheep lungs were homogenized in water (approximately 300 ml) using a commercial bench top blender. Samples of organ homogenate were then analyzed for radiolabel content as described for rat organs.

Feces: Samples of sheep feces (approximately 100 g) collected prior to dosing and at each of the 24 h time periods following dosing were homogenized using a commercial bench top blender to give a feces sample with evenly dispersed radiolabel. The percentage of feces collected on each day out of total collected feces was calculated for each sheep. A sample of feces from each day was then pooled to provide a final sample (500 mg) which comprised of the correct percentage contributions calculated from each day. Two samples of blank feces (500 mg) were also weighed per sheep to provide for background correction in the scintillation counter, and one blank sample per sheep was spiked with a known quantity of radiolabeled dendrimer to calculate the counting efficiency of ^{3}H-dendrimer in sheep feces. This was facilitated by the addition of a similar quantity of ^{3}H-dendrimer into a vial without feces. Water (20 ml) was then added to each sample, as well as to an empty vial (not containing feces or dendrimer) and all samples were vortexed and left at room temperature for 24 h to solubilize the feces. The samples were then vortexed again and centrifuged (4053*g* for 10 min) to pellet solid material, and triplicate aliquots (2 ml) of supernatant were collected and mixed with 500 µl hydrogen peroxide. Samples were then vortexed with Irga-Safe (10 ml) and cooled in the dark for 4 days at 4°C prior to being analyzed for tritium via liquid scintillation counting. The extraction/counting efficiency of radiolabel from the feces samples was determined as previously reported [16] according to Eq. (1):

$$\text{efficiency} = \frac{\text{spikedfeces}_{\text{dpm}} - \text{feces}_{\text{dpm,uncorr}}}{\text{spikedsolution}_{\text{dpm}}} \quad (1)$$

where $spiked\ feces_{dpm}$ is the radioactivity of blank feces samples spiked with known amounts of dendrimer, $feces_{dpm,uncorr}$ is the radioactivity of feces samples, and $spiked\ solution_{dpm}$ is the radioactivity of vials without feces that were spiked with a known amount of dendrimer. This efficiency value was then used to correct the ^{3}H content of feces samples according to Eq. (2):

$$\text{feces}_{\text{dpm,corr}} = \frac{\text{feces}_{\text{dpm,uncorr}}}{\text{efficiency}} \quad (2)$$

where $feces_{dpm,corr}$ is the radioactivity of the feces sample corrected for extraction efficacy. The mass of the total feces excreted was then used to determine the total amount of radiolabel present in the feces of each sheep.

Analysis of the Size of ^{3}H Species in Biological Samples via Size Exclusion Chromatography

In order to evaluate whether biological samples collected at different time points contained intact dendrimer or low MW products of dendrimer degradation after IV and pulmonary administration to rats and sheep, samples of urine, BALF and the supernatant from lung tissue homogenate were analyzed via size exclusion chromatography (SEC) with post-column fraction collection. All samples were centrifuged (500*g* for 5 min) and the supernatant was filtered with Ultrafree®-MC 22 µm centrifuge filters (Merck Millipore, HE, Germany). A Waters 717 Plus Autosampler (Waters; NSW, Australia) and Waters 610 Fluid Unit (Waters; NSW, Australia) were used to inject filtered samples (200 µl) onto a Superdex 75 10/300 GL size exclusion column (GE Healthcare, NSW, Australia). Samples were eluted at a flow rate of 0.5 ml/min in a mobile phase of phosphate buffered saline with 0.3 M NaCl (pH 3.5). Column eluate was collected into 6 ml scintillation vials at 1 min intervals using a Gilson FC 203B Fraction Collector (Gilson Inc., WI, USA). Samples were vortexed mixed with Irga-Safe (2 ml) and analyzed for radiolabel content via liquid scintillation counting.

Non-Compartmental Pharmacokinetic Analysis

The concentration of dendrimer in biological samples was calculated based on the specific radioactivity of the construct and was used to evaluate the pharmacokinetic parameters. This data should be interpreted with the caveat, however, that concentrations are based on the assumption that all radiolabel is associated with intact dendrimer. As described in subsequent sections, the radioactivity measured is not always representative of intact dendrimer alone since the poly(lysine) structure is subject to biodegradation *in vivo*.

Non-compartmental pharmacokinetic parameters were calculated using Phoenix® 64 WinNonlin® software (Version 6.3, Certara®, MO, USA). Calculated pharmacokinetic parameters included the elimination rate constant (k), plasma half-life ($t_{1/2}$), maximum plasma concentration (C_{max}), time to maximum plasma concentration (T_{max}), area under the plasma concentration-time curve (AUC), area under the first moment curve (AUMC), plasma clearance (CL), volume of steady state distribution (V_{ss}), fraction of radiolabel dose absorbed into the blood (F_{blood}) and fraction of administered radiolabel dose recovered in the lymph (F_{lymph}).

Statistics

Differences between pharmacokinetic parameters of rats and sheep in corresponding treatment groups, between rats dosed with spray or liquid instillation and between pulmonary dosed and lymph cannulated sheep were compared using unpaired

t-tests. Unpaired t-tests were also used to evaluate statistical differences between dendrimer concentrations in sheep plasma and lymph and between rat and sheep organ biodistribution. Significance was tested at a confidence level of $\alpha = 0.05$, and significance concluded when $p < 0.05$.

RESULTS

Comparison of the Pulmonary Pharmacokinetics of Dendrimer in Rats After Administration via Liquid Instillation and Aerosol Microsprayer

In a previous study, we reported the pharmacokinetics of $lys_{16}(PEG_{570})_{32}$ following liquid instillation to the lungs of rats [17]. In the current study, we re-evaluated the pulmonary pharmacokinetics of the dendrimer after aerosol administration to better reflect the nebulized administration of dendrimer to the lungs of sheep and to allow a more accurate comparison of pharmacokinetic behavior between the two species. A comparison of the plasma concentration-time profiles of the dendrimer after administration via liquid instillation (data reproduced from reference [17]) and via aerosol microsprayer is shown in Fig. 3.

After pulmonary administration, the T_{max} of the dendrimer was comparable across the two administration methods (approximately 13 h). In contrast, C_{max} following liquid instillation was approximately 3 times greater than that observed after aerosol administration ($p < 0.05$). Due to the different sample collection times between the two studies (2 days after liquid instillation in previous studies rather than the longer sampling strategy adopted here (7 days) after aerosol administration), a comparison of the elimination profiles was not possible. In general, however, administration via liquid instillation appeared to increase absorption and systemic exposure, at least up to 48 h post dose.

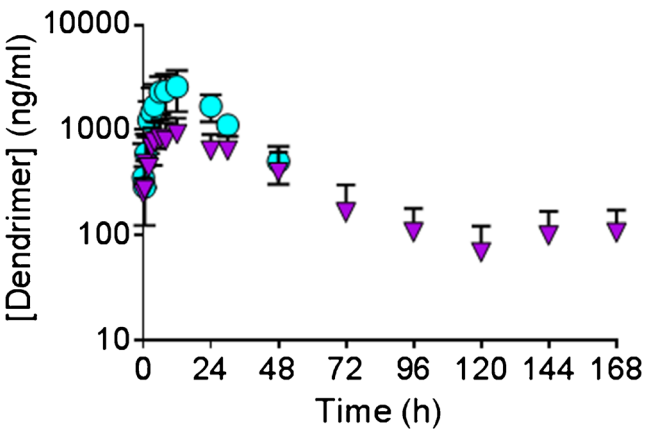

Fig. 3 Plasma-concentration time profiles of dendrimer administered to the lungs of rats via liquid instillation (*blue circles*) or aerosol microsprayer (*purple inverted triangles*). Animals were administered a nominal dose of 5 mg/kg dendrimer in a volume of 100 μl. Data represents mean ± SD ($n = 4$).

Plasma Pharmacokinetics in Rats and Sheep

The dose normalized (5 mg/kg dendrimer) plasma concentration-time profiles of dendrimer following IV and pulmonary administration in rats and sheep are shown in Fig. 4.

Following IV administration, sheep and rats showed similar plasma pharmacokinetic profiles until approximately 24 h following administration, at which point the plasma clearance of dendrimer from sheep slowed considerably (CL in rats approximately twice the rate of CL in sheep and the plasma AUC was >2-fold higher in sheep when compared to rats (Table II).). The volumes of distribution were nearly identical in rats and sheep. As such the terminal elimination rate constant in IV-dosed rats was approximately 2-fold higher than in IV-dosed sheep.

After pulmonary administration, rats and sheep showed no significant differences in exposure (Fig. 4, Table II). C_{max} values after pulmonary administration in rats and sheep were similar and the bioavailability of the dendrimer following administration to rats was 16 and 9% in sheep. The difference in bioavailability reflected lower clearance in sheep after IV administration when compared to rats (although this difference was not statistically significant).

The plasma pharmacokinetic parameters of dendrimer following pulmonary administration to control (non-lymph cannulated) and to lymph-cannulated sheep was also not statistically different.

Lung Retention and Speciation of Dosed Radiolabel in the Lungs of Rats and Sheep Administered an Aerosol Dose

To understand the fate and lung retention times of dendrimers within the lungs of rats and sheep following pulmonary administration, lung and BALF samples were analysed for radiolabel content and dendrimer stability at various times after dosing. Figure 5 Panel A shows that the amount of radiolabel recovered within the BALF of rats decreased steadily over 7 days, such that less than 3% remained in BALF after 7 days. This was consistent with absorption across the lungs coupled with clearance via the mucociliary elevator. Accordingly, the amount of radiolabel recovered in the lung tissue of rats (Panel B) increased between 1 and 72 h (indicating passage of dendrimer from lung lining fluid into the lung parenchyma), and then remained consistent until 168 h following administration. The proportion of low MW dendrimer fragments that were recovered within both the BALF and lungs of rats increased over time, indicating that the dendrimer showed increased degradation within the lungs over time.

While the proportion of the dose remaining in the BALF of rats could be accurately determined (since the dendrimer in

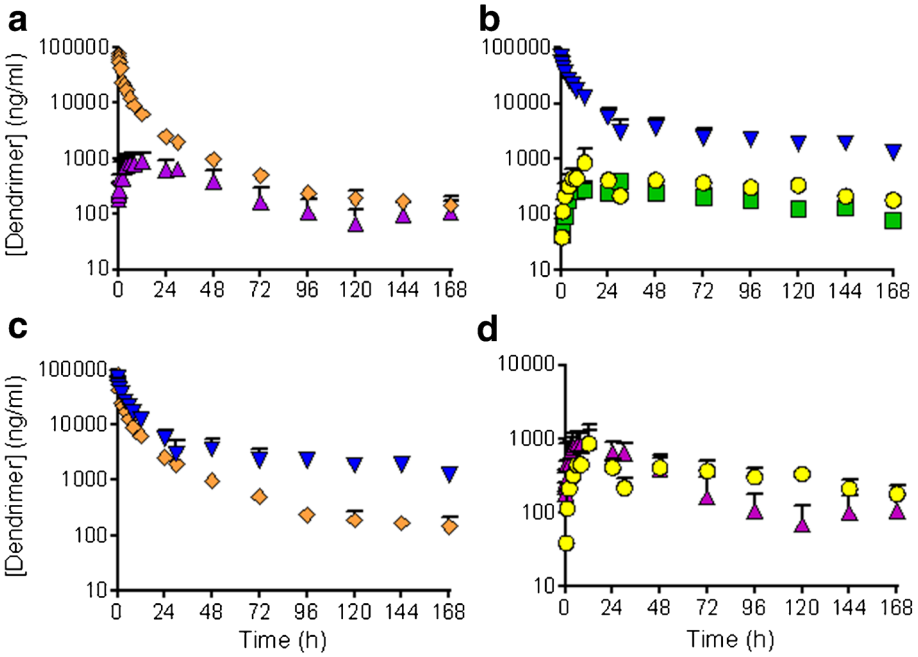

Fig. 4 Plasma concentration-time profiles of dendrimer in rats and sheep following IV and pulmonary administration. Panel **A** – plasma profiles in rat after IV and pulmonary administration. Panel **B** – plasma profiles in sheep after IV and pulmonary administration in lymph-cannulated and control animals. Panel **C** – comparative plasma profiles in rats and sheep after IV administration. Panel **D** – comparative plasma profiles in rats and sheep after pulmonary administration. *Orange diamonds* represent IV-dosed rats, *purple triangles* represent pulmonary-dosed rats, *blue inverted triangles* represent IV-dosed sheep, *yellow circles* represent pulmonary-dosed sheep, and *green squares* represent pulmonary dosed, lymph-cannulated sheep. Data were normalized to a dose of 5 mg/kg dendrimer. Data represents mean ± SD ($n = 3–4$).

the entire BALF content was collected at individual (terminal) time points), in sheep, this was not practical. Similarly, samples of lung tissue were not collected at different time points and thus, lung tissue biodistribution data is shown only after 7 days (Panel D). For BALF, instead of serial killing experiments, representative samples of lung BALF were collected from different regions of the lungs of individual sheep over time and the results are plotted in Fig. 5, Panel C as the proportion of radiolabel recovered at each time. The sample collected at the first sampling point (30 min) was nominally set to represent 100% dose in BALF. The proportion of the aerosol dose in BALF decreased rapidly after aerosol administration such that less than 20% of the nominal dose remained in the BALF after 24 h. BALF sampled from sheep after 7 days was below the accurate level of ^{3}H quantification. Consistent with the rat data, the ratio of low MW products to intact dendrimer present in BALF increased over time (Panel C). Unlike the rat data, at 168 h following administration only 2% of the administered dose was quantified in the lung tissue of sheep and approximately 50% of lung associated radiolabel was present as low molecular weight product (Panel D).

Table II Non-Compartmental Pharmacokinetic Parameters in Non-Lymph Cannulated Rats and Sheep Administered Dendrimer via IV Infusion or Inhalation

	Rat IV	Rat pulmonary	Sheep IV	Sheep pulmonary	Sheep pulmonary + Lymph
k (h^{-1})	0.023 ± 0.004*	0.014 ± 0.005	0.01 ± 0.001	0.009 ± 0.002	0.010 ± 0.001
$t_{1/2}$ (h)	30.8 ± 6.0*	55.7 ± 17.1	70.5 ± 7.9	85.6 ± 23.0	72.2 ± 13.6
C_{max} (mg/L)	NA	0.94 ± 0.39	NA	0.74 ± 0.50	0.46 ± 0.10
T_{max} (h)	NA	13.5 ± 7.6	NA	24.0 ± 20. 8	18.5 ± 13.3
AUC (mg/L/h)	360 ± 22*	58 ± 23	891 ± 267	76 ± 18	41 ± 5
CL (L/h/kg)	0.01 ± 0.001*	NA	0.006 ± 0.002	NA	NA
V_{ss} (L/kg)	0.62 ± 0.09	NA	0.62 ± 0.24	NA	NA
F_{blood} (%)	NA	16 ± 6	NA	9 ± 2	5 ± 0.5

*$P \leq 0.05$, cf. sheep in the same treatment group. Animals were administered a nominal dose of 5 mg/kg dendrimer by IV or pulmonary administration. NA represents parameters that were not calculated. Data represents mean ± SD ($n = 3–4$)

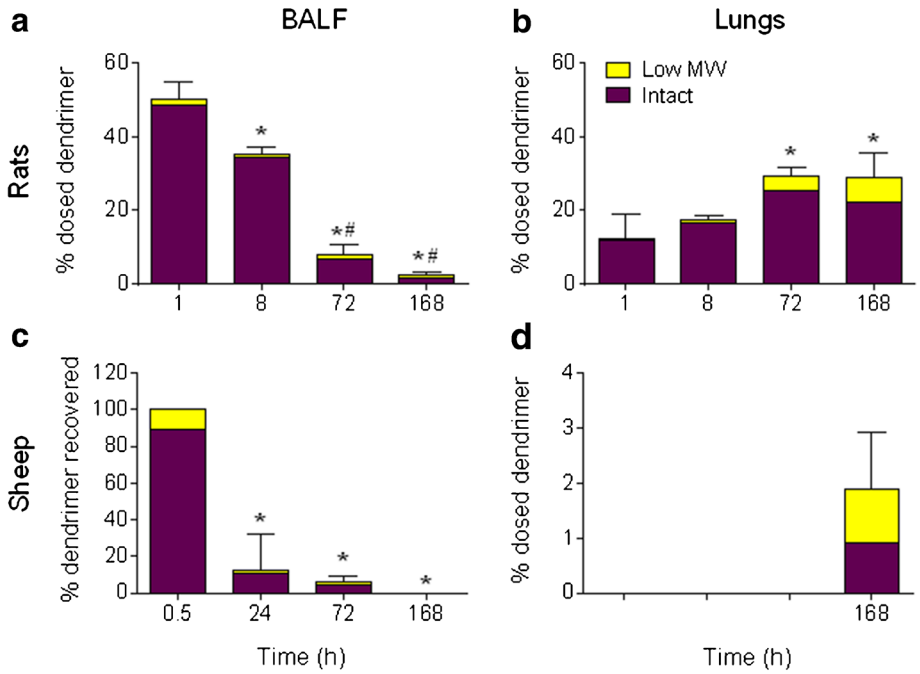

Fig. 5 BALF (Panels **A** and **C**) and lung (Panels **B** and **D**) biodistribution of radiolabel associated with intact dendrimer and low MW product following pulmonary administration of dendrimer in rats (Panels **A** and **B**) and sheep (Panels **C** and **D**). *Dark purple* bars represent intact dendrimer, *yellow* bars represent low MW dendrimer product. Data represents the mean recovery of dosed dendrimer per sample ± SD ($n = 3$–4).

Excretion of Dosed Radiolabel via the Urine and Speciation of Excreted ^{3}H

The excretion of radiolabel in urine was greater following IV rather than with pulmonary administration for both rats and sheep, consistent with greater plasma concentrations at all times following IV administration and limited pulmonary bioavailability. Urinary excretion after IV administration was similar in rats and sheep and approximately 40% of the dose was recovered in urine over 7 days.

The absolute (low) levels of ^{3}H present in plasma in rats and sheep precluded detailed analysis of the species present by SEC. As such, urine samples were analysed instead to give an indirect indication of the relative stability of the dendrimer after IV and pulmonary administration (Fig. 6). The recovery of radiolabel within the urine of rats after 96 h was also too low for speciation via SEC, and so values were only quantified up to this time. Following IV administration, relatively small quantities (5.4 and 4.5% of the dosed radiolabel respectively) were recovered in the urine of rats and sheep as low MW products. This corresponded to 14.5 and 15.6% of total radiolabel in urine in rats and sheep respectively (Fig. 6). Particularly for sheep, the recovery of intact dendrimer in urine diminished over time while the recovery of the low MW dendrimer products was consistent throughout the study, indicating that the relative proportion of breakdown products in urine was increasing over time. In all cases, however, the total quantity of breakdown products was low. In contrast, following pulmonary administration in rats, approximately 40% of the total radiolabel recovered in urine was associated with low MW dendrimer breakdown products (Fig. 6, Panel E). The data suggest that in rats, the majority of dendrimer degradation following pulmonary administration occurred prior to systemic absorption, since only 5.4% of the dose was present in urine as breakdown products after IV administration. Due to the relatively low pulmonary bioavailability of the dendrimer and significant dilution of radiolabel in the larger volume of urine excreted by sheep (approximately 100 fold larger than in rats), the ^{3}H content in sheep urine was too low to facilitate SEC analysis after pulmonary administration.

Organ Biodistribution

To gain further insight into the *in vivo* fate of dendrimers following IV and pulmonary administration, the recovery of the dendrimer in the major organs as well as in the urine and feces was analyzed after IV and pulmonary administration (Fig. 7).

Following IV administration, the biodistribution of the dendrimer was similar in rats and sheep, with the majority of the administered radiolabel recovered in urine and feces over 7 days. Following pulmonary administration, a greater proportion of the total radiolabelled dose was recovered from samples collected from rats, with the exception of the liver where biodistribution was higher in sheep when compared to rats. Approximately 50% of the administered radiolabel was recovered in the feces of rats (although this was highly variable), while only 9% was recovered in the feces of sheep.

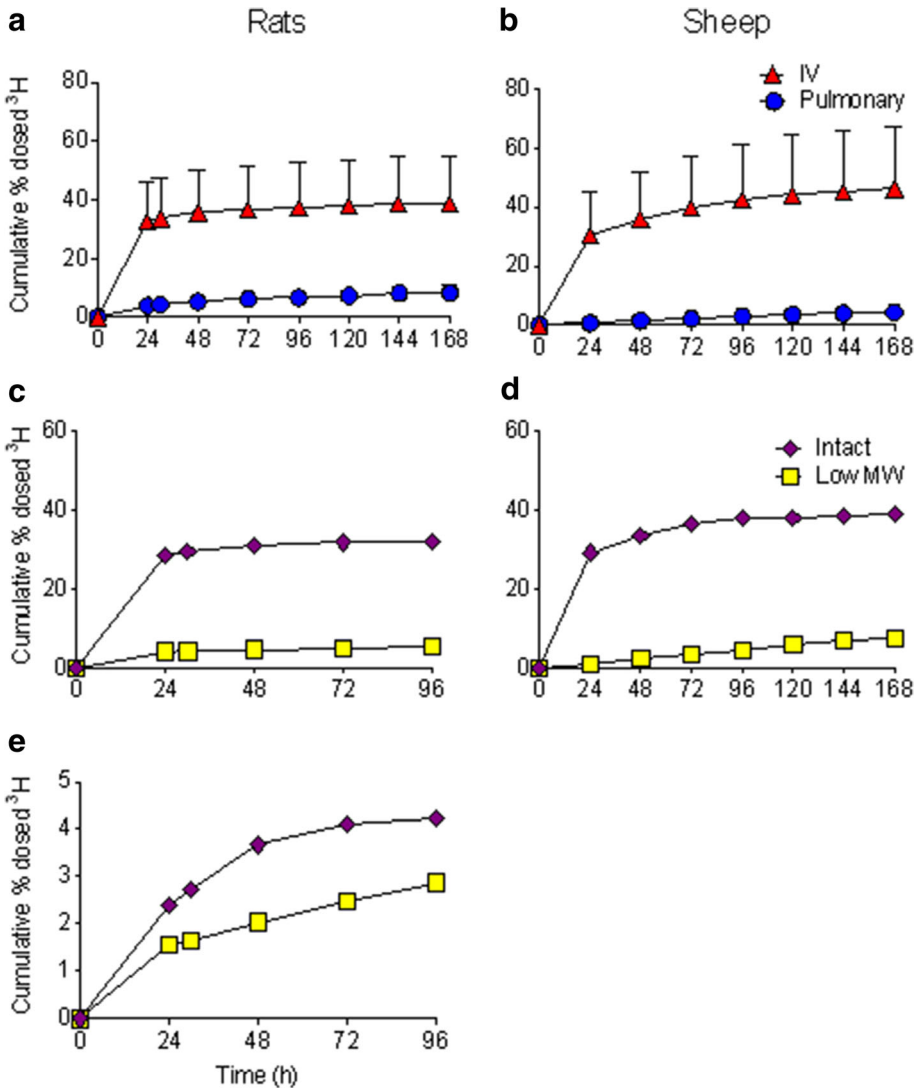

Fig. 6 Cumulative recovery of the ^{3}H-dendrimer dose in urine following IV and pulmonary administration to rats and sheep. Panels **A** and **B** represent the cumulative proportion of dosed radiolabel recovered in urine in rats and sheep respectively, following IV (*red triangles*) and pulmonary (*blue circles*) administration. Panels **C**, **D** and **E** represent the cumulative recovery of radiolabel associated with intact dendrimer (*purple diamonds*) or low MW dendrimer products (*yellow squares*) in urine following IV (Panels **C** and **D**) and pulmonary (Panel **E**) administration in rats (Panels **C** and **E**) and sheep (Panel **D**). Data for Panels **A** and **B** represent mean ± SD ($n = 3$–4).

In addition, approximately 29% of dendrimer dose was recovered within the lungs of rats 7 days after pulmonary administration, whilst only 2% of the administered radiolabel was recovered in the lungs of sheep.

Pulmonary Lymphatic Availability of Dendrimer Following Pulmonary Administration in Sheep

The cumulative recovery of pulmonary dosed dendrimer from the efferent CMLD of sheep is shown in Fig. 8, and was approximately 0.2% after 7 days (Panel A). The concentration of dendrimer recovered within the lymph however, was greater than the concentration within plasma at all observed time points (Panel B), and was statistically greater at 12 h following dendrimer administration. The maximum concentration of radiolabel within lymph occurred at around 12 h following administration, mimicking the T_{max} of dendrimer in the plasma of pulmonary-dosed sheep.

DISCUSSION

There is increasing interest in the development of inhalable nano-sized drug delivery systems as a means of controlling the rate and extent of lung exposure and systemic absorption of associated drugs. Nanoparticle-based delivery systems can be used to promote directed drug delivery to the lungs to treat respiratory disease, or as a conduit to non-invasive delivery of drugs to diseases that reside outside of the lungs. For example, chemotherapy for metastatic lung cancers most commonly involves drug administration via slow IV infusion, but many preclinical and clinical studies have demonstrated that drug administration directly into the lungs can significantly improve treatment outcomes for lung-resident cancers [30–32]. Widespread clinical translation of this approach however, has been limited by extensive local toxicity associated with the inhalation of high concentrations of cytotoxic drugs [31, 33, 34]. In an attempt to address this problem, our previous studies have shown that conjugating doxorubicin to a PEGylated

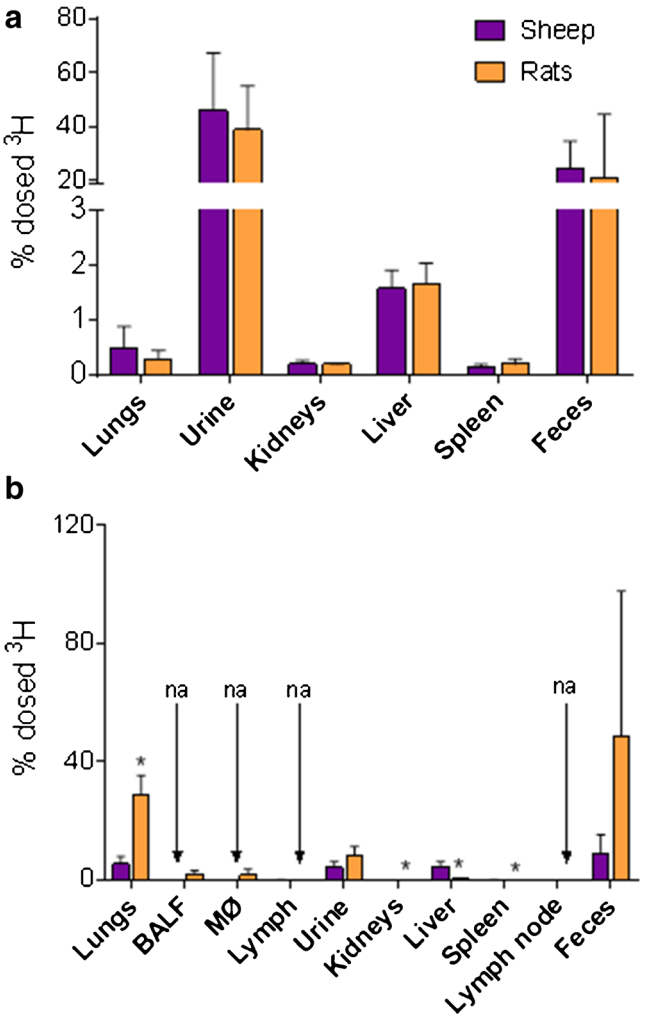

Fig. 7 Biodistribution of dendrimer in major organs, urine, lymph and feces of rats and sheep administered tritiated dendrimer (5 mg/kg) via IV (Panel **A**) or pulmonary (Panel **B**) routes. Data represents mean ± SD ($n = 3$–4). * Represents $p \leq 0.05$ cf. sheep. na represents samples that were not analyzed.

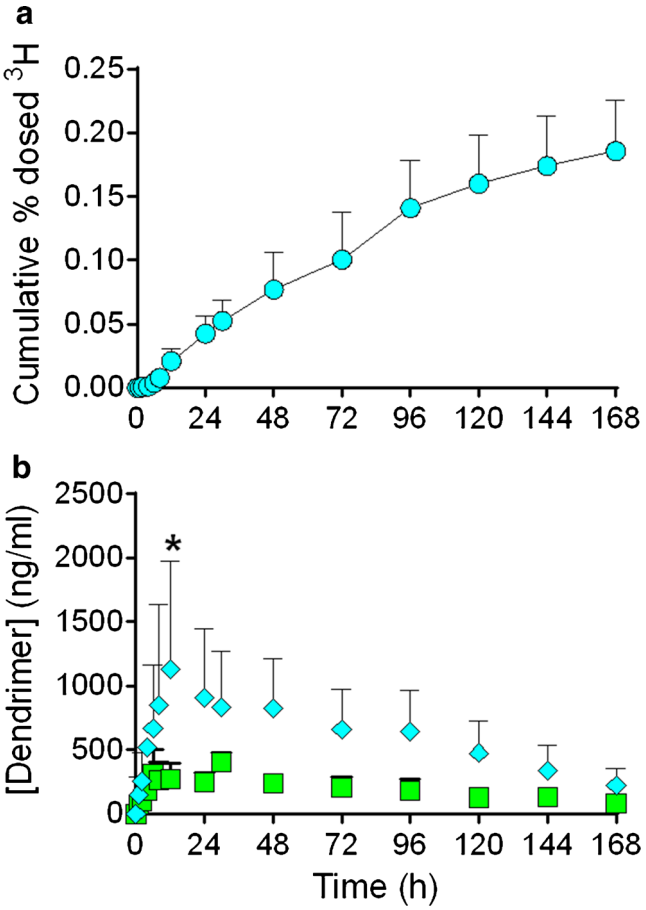

Fig. 8 Recovery of dendrimer in CMLD lymph of sheep after pulmonary administration. Panel **A** represents the cumulative recovery of the ^{3}H dose in efferent CMLN lymph, and Panel **B** represents the concentration of dendrimer in collected lymph (*blue diamonds*) and plasma (*green squares*) over 7 days from lymph-cannulated sheep. * Represents $p \leq 0.05$ compared with plasma concentrations at the same time. Data represents mean ± SD ($n = 3$–4).

poly-lysine dendrimer reduces the lung associated toxicity of doxorubicin after pulmonary administration in rats when compared to the pulmonary administration of a solution formulation [14]. The data also demonstrated more pronounced inhibition of lung tumor growth after administration of the doxorubicin-dendrimer conjugate via the lungs when compared to an equivalent IV dose.

We have also previously shown that after intratracheal liquid instillation a 22 kDa PEGylated dendrimer gains access to the interstitium within the lungs [17] and is absorbed from interstitial SC injection sites largely via the lymph [6]. These observations led to the hypothesis examined here - that the pulmonary lymphatic system plays a significant role in the absorption of PEGylated dendrimers from the lungs. The current study was undertaken to probe this hypothesis and to evaluate the pulmonary lymphatic pharmacokinetics of the 22 kDa PEGylated dendrimer used previously, in an animal model (sheep) that has a respiratory physiology that closely matches that of humans. Identification of drug delivery vehicles that promote access to lung lymph after inhaled administration has the potential to enhance the treatment of lung cancer, and in particular, lung lymphatic metastases. In parallel, we sought to better understand differences in the pharmacokinetic behavior of the dendrimer after liquid instillation and aerosol administration in rats (which are commonly used as preclinical pharmacokinetic models) and after inhalation of an aerosolized solution in sheep. This is an important step in better understanding the potential to translate inhalable nanomedicines from rodents into humans. It is important to note, however, that the PEGylated surface on the dendrimer examined here likely increased the observed hydrodynamic radius due to extensive absorption of water when compared to proteins of similar molecular weight [35]. Thus, the 22 kDa dendrimer used here (11 nm diameter) [6] has a similar hydrodynamic radius to a 150 kDa antibody.

The data presented here show that liquid instillation of the dendrimer to the lungs of rats results in a higher plasma C_{max} than that obtained after administration of an aerosol (Fig. 3).

This contradicts much of the literature which suggests that drug bioavailability is greater following delivery of an aerosolized dose when compared to liquid instillation [36, 37]. While unlikely given the dimensions of the rat respiratory track and aerosol particle size generated by the microsprayer, it is possible that a proportion of the aerosolized dose delivered via the microsprayer may have been exhaled, resulting a lower plasma C_{max}. Unfortunately, however, it is not possible to capture and accurately quantify the proportion of an aerosolized dose exhaled from rats since the microsprayer is not a 'closed system'. This is a notable limitation in using rodents as a model for pulmonary pharmacokinetic studies. Consistent with the present data, however, a similar observation was reported previously for parathyroid hormone administered via liquid instillation rather than an aerosol to the lungs of rats [38]. In the parathyroid hormone study administration via liquid instillation resulted in a C_{max} up to 4 times greater than that achieved after aerosol administration. The authors suggested that this reflected different disposition patterns of parathyroid hormone within the lungs, where administration via liquid instillation resulted in greater deep lung penetration, whereas greater recovery within the trachea was evident following aerosol administration. The volume of liquid deposited at the top of the lungs following liquid instillation may also cause localized dilution of the lung surfactant layer, increasing permeability across the airways to the systemic circulation.

Subsequent work sought to compare the pharmacokinetics of the dendrimer in rats and sheep. The plasma pharmacokinetics of the dendrimer following IV administration were similar in sheep and rats for the first 24 h, but at later times dendrimer clearance was reduced in sheep. This is consistent with a large body of work suggesting that in general, clearance in smaller animals is faster than that in than larger animals [39]. In contrast, following aerosolized administration and despite differences in animal size, the dose normalized pharmacokinetic parameters of the dendrimer in sheep and rats were not significantly different across all time periods. In general, the similarities in pharmacokinetics across species suggest that the rat model may be utilized to evaluate how the physicochemical properties of nano-sized drug delivery systems impact upon patterns of lung clearance, such as absorption kinetics, after inhaled administration (realizing that liquid instillation may overestimate absorption to a degree and that some differences in clearance may be evident).

Over the course of 7 days, the mass of pulmonary administered radiolabel recovered within the BALF of rats (i.e., on the air side of the lungs) decreased, and the amount recovered in lung tissue homogenate increased. The ratio of low MW dendrimer products to intact dendrimer also increased within rat BALF and lung tissue as a function of time. The data suggest gradual absorption and breakdown of dendrimer within the lungs. The removal of radiolabel from the lungs likely occurred via systemic absorption (16% pulmonary bioavailability) and mucociliary clearance (50% administered dendrimer recovered within feces). The absorption of low MW dendrimer fragments into blood (as suggested by the SEC profiles of rat and sheep urine) also suggests that the calculated bioavailability of the dendrimer following pulmonary administration in rats and sheep is over-estimated.

Low MW dendrimer fragments were also evident within the lungs of sheep, however only 2% of the dose was retained in sheep lungs 7 days post dose when compared with approximately 30% in rats. These data suggest more effective lung clearance mechanisms in sheep when compared to rats. The greater airway clearance observed in sheep may stem from an ability to cough (as is seen in humans), a reflex that does not exist in rodents [40]. This has been shown previously to significantly increase the rate of clearance of inhaled particles from healthy lungs in humans [41, 42]. The cough reflex, however, is expected to facilitate dendrimer transfer from the lungs into the mouth and throat, resulting in excretion in feces. Fecal recovery of radioactivity in sheep (9% of administered radiolabel), however, was significantly lower than in rats (50% of administered radiolabel). This suggests that the low recovery of radioactivity in the lung at later time points in the sheep is not due to coughing or mucociliary clearance. Unlike rats (and indeed humans) sheep are ruminants with a series of stomachs that are responsible for the digestion of cellulose-based food. It is therefore possible that ingested poly(lysine) dendrimer (which has a protein-like structure) was degraded within the rumen [43] resulting in the generation of ^{3}H-lysine fragments that may have been absorbed rather than excreted in feces. In this scenario, however, the concentrations of radiolabel in plasma might be expected to increase as the radiolabelled fragments were absorbed. This was not readily apparent in the plasma data. A full explanation for the low total recovery of radiolabel in the sheep, bearing in mind low recovery in feces and urine is not clear at this time.

Finally, we sought to evaluate the contribution of the pulmonary lymphatic system to the systemic absorption of the dendrimer from the sheep lung. Lung lymph sampling was achieved by chronic cannulation of the efferent CMLD. While cannulation of this vessel allows for the collection of a large proportion of lymph formed in the lungs, it is not practical to collect all lung lymph fluid since pulmonary lymph drains into blood via two main lymph ducts - the right lymph duct and the thoracic duct (into which CMLD lymph flows). Nonetheless, it has been estimated that approximately 60% of lymph fluid formed in the lungs of sheep drains via the CMLD into thoracic lymph [44]. Despite the collection of approximately half of the lymph formed in the lungs, total lung lymphatic recovery of the pulmonary dendrimer dose was less than 0.5% of the total administered dose. This is an insignificant amount when compared with the recovery of approximately 30% of the dendrimer in thoracic duct lymph

following SC administration in rats [6]. This suggests that the pulmonary lymphatic system is unlikely to play a significant role in the clearance of inhaled nanocarriers from the lungs of large animals and humans. The greater concentration of tritium recovered within the lymph of sheep in comparison to the plasma does, however, suggest that a large portion of the dendrimer recovered within the lymph in this study was the result of direct lymphatic drainage from the lungs, rather than redistribution of dendrimer from systemic circulation into lymph as described previously in rats [6].

Previous data has shown that the lymphatic absorption of PEGylated dendrimers following SC administration is significant and that pulmonary bioavailability, at least in rats, is relatively high. We therefore expected a considerable portion of the dose that was absorbed from the lungs of sheep to be recovered within the lymph. This was not the case. The discrepancy between lymphatic recovery of the dendrimer following pulmonary and SC administration likely stems from the distribution of lymphatic vessels within each of these absorptive sites. Dendrimer absorption from the lungs most likely occurred via the alveolar region. However, alveoli lack or possess minimal lymphatic vasculature [45]. In contrast, most of the lymphatic structures in the lungs occur around the upper airways and pleura, with some small lymphatic collecting ducts residing around interalveolar scepta. As such, the small amount of dendrimer recovered from CMLD lymph is likely to result from considerable absorption via the more permeable alveolar regions where the numbers of lymph vessels are low, or via limited absorption across in areas where lymphatic vessels are present but where lung permeability is low (thereby limiting the absolute extent of absorption) [1].

Interestingly, this is in contrast to findings by others in rats using less quantitative approaches. For instance, using near infrared fluorescence imaging, Choi *et al.* [46] demonstrated that quantum-dot nanoparticles of comparable size (7 nm hydrodynamic diameter) to the dendrimer used in this study were translocated from the lungs of rats to mediastinal lymph nodes very rapidly (3 min). At 1 h post dose 2.18% of the injected dose of nanoparticles /g lymph node (approximately 0.02% of total dose based on an average rat lymph node weight of 10 mg in rats) was recovered in the mediastinal lymph nodes. By comparison, in the current study approximately 0.004% of the dosed dendrimer (0.005% total dose/g) was recovered within the CMLN of pulmonary-dosed sheep 7 days following aerosol administration. Choi and colleagues concluded that in general, nanoparticles <34 nm in diameter and those without cationic surface charge were significantly absorbed via the lung lymphatics in rats (although the absolute levels were still low). However, nanoparticles are likely to have easier access to lung lymph in rodents than in larger animals, since nanoparticles must translocate further in large animals to gain access to lymphatic structures. This raises questions about the use of rodents to indicate lung lymphatic exposure of inhaled nanoparticles in humans. It also suggests that more sophisticated targeting approaches may be needed to improve the delivery of nanomedicines and nano-sized imaging agents to the lung lymphatics after inhaled administration.

Matthay *et al.* [47] have previously described significant exposure of albumin in lung lymph after pulmonary delivery to sheep. To the best of our knowledge this is the only study (other than the data reported here) that has quantified the lymphatic availability of a pulmonary delivered macromolecule. In the Matthay study, a lymph vessel cannulation technique similar to that used in the current study was used to quantify the pulmonary lymphatic recovery of human serum albumin following liquid instillation to the lungs [47]. Approximately 30% of the albumin dose was recovered in the pulmonary lymphatics up to 48 h post dose. Similar to the present study, lymph-albumin concentrations peaked 12–17 h following instillation. The significant difference in lung-lymph recovery between this and the current study may be a result of active transport (absorption) of albumin from the lungs since clathrin-dependent endocytosis mediated by the megalin receptor has been shown to be at least partly responsible for albumin absorption across the alveolar epithelium [48]. This suggests that nanocarriers that bind to albumin in the alveolar lining fluid may be more effectively absorbed. Drug association with albumin was recently shown to dramatically improve the lymphatic transport of molecular vaccines following SC administration [9], although whether albumin is able to act as a carrier for much larger nanoparticles is not clear.

CONCLUSION

The current study explored the pharmacokinetics of a fully PEGylated lysine dendrimer following IV and pulmonary administration in sheep and rats. Despite numerous physiological differences between ovine and rodent models, the plasma pharmacokinetics of the dendrimer were similar across the animal models following IV and pulmonary administration. This suggests that rats are an appropriate and high-throughput small animal model to evaluate how differences in nanoparticle properties impact upon pulmonary pharmacokinetics. Definitive conclusions regarding the relevance of either model to dendrimer disposition in humans, however, are difficult without comparative human data sets. A potential shortcoming of the sheep model is the discrepancy between human and ovine digestive systems. This becomes relevant in pulmonary delivery studies when a significant proportion of the dose is cleared from the lungs and swallowed. In contrast, the sheep provides advantage in allowing more effective aerosolized administration and also allowing sampling of lung lymph. This provided one of the first quantitative assessments of the pulmonary lymphatic bioavailability of a nano-sized

material in an animal model that has a similar respiratory physiology to humans. However, less than 0.5% of the pulmonary administered dendrimer was recovered within the pulmonary lymph, despite qualitative studies in rats suggesting that nanomaterials of this size should efficiently gain access to the lung lymphatics after pulmonary administration. This raises questions regarding the use of rodents in lung lymph bioavailability studies, and suggests that nanoparticles may not access the lung lymph in significant quantities after inhaled administration. Systemic absorption directly via the blood therefore appears to be the major contributor to the plasma exposure of the PEGylated dendrimer examined here following pulmonary administration.

ACKNOWLEDGMENTS AND DISCLOSURES

This work was funded by a strategic Monash research grant and an Australian Research Council Linkage grant. LMK was supported by a NHMRC Career Development Fellowship (APP1022732). GMR was supported by a Cancer Council Victoria Postgraduate Scholarship.

REFERENCES

1. Patton JS, Fishburn CS, Weers JG. The lungs as a portal of entry for systemic drug delivery. Proc Am Thorac Soc. 2004;1(4):338–44.
2. Patton JS, Byron PR. Inhaling medicines: delivering drugs to the body through the lungs. Nat Rev Drug Discov. 2007;6(1):67–74.
3. Torchilin VP. Multifunctional nanocarriers. Adv Drug Deliv Rev. 2012;64:302–15.
4. McLeod VM, Chan LJ, Ryan GM, Porter CJH, Kaminskas LM. Optimal PEGylation can improve the exposure of interferon in the lungs following pulmonary administration. J Pharm Sci. 2015;104(4):1421–30.
5. Baginski L, Gobbo OL, Tewes F, Salomon JJ, Healy AM, Bakowsky U, *et al.* In vitro and in vivo characterisation of PEG-lipid-based micellar complexes of salmon calcitonin for pulmonary delivery. Pharm Res. 2012;29(6):1425–34.
6. Kaminskas LM, Kota J, McLeod VM, Kelly BD, Karellas P, Porter CJH. PEGylation of polylysine dendrimers improves absorption and lymphatic targeting following SC administration in rats. J Control Release. 2009;140(2):108–16.
7. Ryan GM, Kaminskas LM, Porter CJH. Nano-chemotherapeutics: Maximising lymphatic drug exposure to improve the treatment of lymph-metastatic cancers. J Control Release. 2014.
8. Tiantian Y, Wenji Z, Mingshuang S, Rui Y, Shuangshuang S, Yuling M, *et al.* Study on intralymphatic-targeted hyaluronic acid-modified nanoliposome: influence of formulation factors on the lymphatic targeting. Int J Pharm. 2014;471(1–2):245–57.
9. Liu H, Moynihan KD, Zheng Y, Szeto GL, Li AV, Huang B, *et al.* Structure-based programming of lymph-node targeting in molecular vaccines. Nature. 2014;507(7493):519–22.
10. Ryan GM, Kaminskas LM, Bulitta JB, McIntosh MP, Owen DJ, Porter CJH. PEGylated polylysine dendrimers increase lymphatic exposure to doxorubicin when compared to PEGylated liposomal and solution formulations of doxorubicin. J Control Release. 2013;172(1):128–36.
11. Kourtis IC, Hirosue S, de Titta A, Kontos S, Stegmann T, Hubbell JA, *et al.* Peripherally administered nanoparticles target monocytic myeloid cells, secondary lymphoid organs and tumors in mice. PLoS ONE. 2013;8(4):e61646.
12. Khullar OV, Griset AP, Gibbs-Strauss SL, Chirieac LR, Zubris KAV, Frangioni JV, *et al.* Nanoparticle migration and delivery of paclitaxel to regional lymph nodes in a large animal model. J Am Coll Surg. 2012;214(3):328–37.
13. Kim CK, Han JH. Lymphatic delivery and pharmacokinetics of methotrexate after intramuscular injection of differently charged liposome-entrapped methotrexate to rats. J Microencapsul. 1995;12(4):437–46.
14. Kaminskas LM, McLeod VM, Ryan GM, Kelly BD, Haynes JM, Williamson M, *et al.* Pulmonary administration of a doxorubicin-conjugated dendrimer enhances drug exposure to lung metastases and improves cancer therapy. J Control Release. 2014;183:18–26.
15. Kaminskas LM, Boyd BJ, Karellas P, Krippner GY, Lessene R, Kelly B, *et al.* The impact of molecular weight and PEG chain length on the systemic pharmacokinetics of PEGylated poly l-lysine dendrimers. Mol Pharm. 2008;5(3):449–63.
16. Boyd BJ, Kaminskas LM, Karellas P, Krippner G, Lessene R, Porter CJ. Cationic poly-L-lysine dendrimers: pharmacokinetics, biodistribution, and evidence for metabolism and bioresorption after intravenous administration to rats. Mol Pharm. 2006;3(5):614–27.
17. Ryan GM, Kaminskas LM, Kelly BD, Owen DJ, McIntosh MP, Porter CJH. Pulmonary administration of PEGylated polylysine dendrimers: absorption from the lung versus retention within the lung is highly size-dependent. Mol Pharm. 2013;10(8):2986–95.
18. Cryan S-A, Sivadas N, Garcia-Contreras L. In vivo animal models for drug delivery across the lung mucosal barrier. Adv Drug Deliv Rev. 2007;59(11):1133–51.
19. Abraham WM. Modeling of asthma, COPD and cystic fibrosis in sheep. Pulm Pharmacol Ther. 2008;21(5):743–54.
20. Meeusen EN, Snibson KJ, Hirst SJ, Bischof RJ. Sheep as a model species for the study and treatment of human asthma and other respiratory diseases. Drug Discov Today: Dis Model. 2009;6(4):101–6.
21. Albertine KH. Progress in understanding the pathogenesis of BPD using the baboon and sheep models. Semin Perinatol. 2013;37(2):60–8.
22. De Las Heras Guillamón M, Borderías Clau L. The sheep as a large animal experimental model in respiratory diseases research. Arch Bronconeumol. 2010;46(10):499–501.
23. Scheerlinck J-PY, Snibson KJ, Bowles VM, Sutton P. Biomedical applications of sheep models: from asthma to vaccines. Trends Biotechnol. 2008;26(5):259–66.
24. Schlesinger RB. Comparative deposition of inhaled aerosols in experimental animals and humans: a review. J Toxicol Environ Health. 1985;15(2):197–214.
25. Staub NC, Bland RD, Brigham KL, Demling R, Erdmann Iii AJ, Woolverton WC. Preparation of chronic lung lymph fistulas in sheep. J Surg Res. 1975;19(5):315–20.
26. Enkhbaatar P, Murakami K, Shimoda K, Mizutani A, Traber L, Phillips GB, *et al.* The iNOS inhibitor, BBS-2 prevents acute lung injury in sheep after burn and smoke inhalation injury. Am J Respir Crit Care Med. 2003;167:1021–6.
27. Caliph SM, Shackleford DM, Ascher DB, Kaminskas LM. Practical lessons in murine thoracic lymph duct cannulations: observations in female and male mice across four different strains that impact on "cannulatability". J Pharm Sci. 2015;104(3):1207–9.
28. Slatter JG, Adams LA, Bush EC, Chiba K, Daley-Yates PT, Feenstra KL, *et al.* Pharmacokinetics, toxicokinetics, distribution, metabolism and excretion of linezolid in mouse, rat and dog. Xenobiotica. 2002;32(10):907–24.

29. Prankerd RJ, Nguyen T-H, Ibrahim JP, Bischof RJ, Nassta GC, Olerile LD, *et al.* Pulmonary delivery of an ultra-fine oxytocin dry powder formulation: potential for treatment of postpartum haemorrhage in developing countries. PLoS ONE. 2013;8(12):e82965.
30. Hershey AE, Kurzman ID, Forrest LJ, Bohling CA, Stonerook M, Placke ME, *et al.* Inhalation chemotherapy for macroscopic primary or metastatic lung tumors: proof of principle using dogs with spontaneously occurring tumors as a model. Clin Cancer Res. 1999;5(9): 2653–9.
31. Zarogoulidis P, Chatzaki E, Porpodis K, Domvri K, Hohenforst-Schmidt W, Goldberg EP, *et al.* Inhaled chemotherapy in lung cancer: future concept of nanomedicine. Int J Nanomed. 2012;7: 1551–72.
32. Gagnadoux F, Pape AL, Lemarié E, Lerondel S, Valo I, Leblond V, *et al.* Aerosol delivery of chemotherapy in an orthotopic model of lung cancer. Eur Respir J. 2005;26(4):657–61.
33. Wittgen BPH, Kunst PWA, van der Born K, van Wijk AW, Perkins W, Pilkiewicz FG, *et al.* Phase I study of aerosolized SLIT cisplatin in the treatment of patients with carcinoma of the lung. Clin Cancer Res. 2007;13(8):2414–21.
34. Otterson GA, Villalona-Calero MA, Sharma S, Kris MG, Imondi A, Gerber M, *et al.* Phase I study of inhaled doxorubicin for patients with metastatic tumors to the lungs. Clin Cancer Res. 2007;13(4):1246–52.
35. Protein purification: principles, high resolution methods, and applications. 3rd ed. Janson J-C, editor: Wiley; 2012.
36. Colthorpe P, Farr SJ, Taylor G, Smith IJ, Wyatt D. The pharmacokinetics of pulmonary-delivered insulin: a comparison of intratracheal and aerosol administration to the rabbit. Pharm Res. 1992;9(6):764–8.
37. Niven RW, Whitcomb KL, Shaner L, Ip AY, Kinstler OB. The pulmonary absorption of aerosolized and intratracheally instilled rhG-CSF and monoPEGylated rhG-CSF. Pharm Res. 1995;12(9):1343–9.
38. Codrons V, Vanderbist F, Ucakar B, Préat V, Vanbever R. Impact of formulation and methods of pulmonary delivery on absorption of parathyroid hormone (1–34) from rat lungs. J Pharm Sci. 2004;93(5):1241–52.
39. Mordenti J. Man versus beast: pharmacokinetic scaling in mammals. J Pharm Sci. 1986;75(11):1028–40.
40. Belvisi MG, Hele DJ. Animal models of cough. In: Chung FK, Boushey H, Widdicombe J, editors. Cough: causes, mechanisms and therapy: Wiley Online Library; 2007.
41. Bennett WD, Foster WM, Chapman WF. Cough-enhanced mucus clearance in the normal lung. J Appl Physiol. 1990;69(5):1670–5.
42. Hasani A, Pavia D, Agnew J, Clarke S. Regional lung clearance during cough and forced expiration technique (FET): effects of flow and viscoelasticity. Thorax. 1994;49(6):557–61.
43. van der Wal JG, Meyer JHF. Protein digestion in ruminants. S Afr J Anim Sci. 1988;18(1):30–41.
44. Chanana AD, Joel DD. The ovine bronchopulmonary lymph drainage pathways: a model to study pulmonary immune responses. Exp Lung Res. 1985;9(3–4):211–20.
45. Schraufnagel DE. Lung lymphatic anatomy and correlates. Pathophysiology. 2010;17(4):337–43.
46. Choi HS, Ashitate Y, Lee JH, Kim SH, Matsui A, Insin N, *et al.* Rapid translocation of nanoparticles from the lung airspaces to the body. Nat Biotechnol. 2010;28(12):1300–3.
47. Matthay MA, Berthiaume Y, Albertine KH, Grady M, Fick G. Protein clearance from the air spaces and lungs of unanesthetized sheep over 144 h. J Appl Physiol. 1989;67(5):1887–97.
48. Buchackert Y, Rummel S, Vohwinkel CU, Gabrielli NM, Grzesik BA, Mayer K, *et al.* Megalin mediates transepithelial albumin clearance from the alveolar space of intact rabbit lungs. J Physiol. 2012;590(Pt 20):5167–81.